DOI : 10.1097/SHK.0000000000001414

Endothelin A and B receptors: potential targets for microcirculatory-mitochondrial therapy in experimental sepsis

Attila Rutai[1], Roland Fejes[1], László Juhász[1], Szabolcs Péter Tallósy[1], Marietta Zita Poles[1], Imre Földesi[2], András T. Mészáros[1], Andrea Szabó[1], Mihály Boros[1], József Kaszaki[1]

[1]Institute of Surgical Research, University of Szeged, Szeged, Hungary

[2]Department of Laboratory Medicine, University of Szeged, Hungary

Running head: Endothelin receptors in sepsis therapy

Corresponding author: József Kaszaki PhD

Institute of Surgical Research, University of Szeged

H-6724 Szeged, Pulz u. 1., Hungary

Tel.: +36 62 545-103

Fax: +36 62 545-743

e-mail: kaszaki.jozsef@med.u-szeged.hu

Attila Rutai and Roland Fejes contributed equally to this article.

Conflict of interest: none declared

ABSTRACT

The hypoxia-sensitive endothelin (ET) system plays an important role in circulatory regulation through vasoconstrictor ET_A and ET_{B2} and vasodilator ET_{B1} receptors. Sepsis progression is associated with microcirculatory and mitochondrial disturbances along with tissue hypoxia. Our aim was to investigate the consequences of treatments with the ET_A receptor (ET_A-R) antagonist, ET_{B1} receptor (ET_{B1}-R) agonist, or their combination on oxygen dynamics, mesenteric microcirculation and mitochondrial respiration in a rodent model of sepsis. Sprague Dawley rats were subjected to fecal peritonitis (0.6 g kg^{-1} ip) or a sham operation. Septic animals were treated with saline or the ET_A-R antagonist ETR-p1/fl peptide (100 nmol kg^{-1} iv), the ET_{B1}-R agonist IRL-1620 (0.55 nmol kg^{-1} iv), or a combination therapy 22 h after induction. Invasive hemodynamic monitoring and blood gas analysis were performed during a 90-min observation, plasma ET-1 levels were determined, and intestinal capillary perfusion (CPR) was detected by intravital videomicroscopy. Mitochondrial Complex I (CI)- and CII-linked oxidative phosphorylation (OXPHOS) was evaluated by high-resolution respirometry in liver biopsies. Septic animals were hypotensive with elevated plasma ET-1. The ileal CPR, oxygen extraction (ExO_2), and CI–CII-linked OXPHOS capacities decreased. ETR-p1/fl treatment increased ExO_2 (by >45%), CPR, and CII-linked OXPHOS capacity. The administration of IRL-1620 countervailed the sepsis-induced hypotension (by >30%), normalized ExO_2, and increased CPR. The combined ET_A-R antagonist–ET_{B1}-R agonist therapy reduced the plasma ET-1 level, significantly improved the intestinal microcirculation (by >41%), and reversed mitochondrial dysfunction. The additive effects of a combined ET_A-R–ET_{B1}-R-targeted therapy may offer a tool for a novel microcirculatory and mitochondrial resuscitation strategy in experimental sepsis.

Keywords: fecal peritonitis, endothelin receptors, oxygen extraction, microcirculation, mitochondrial respiration, resuscitation, rat

INTRODUCTION

Sepsis is a potentially life-threatening condition caused by a dysregulated host response to an infection (1). Along with its progression, the regulatory failure is frequently associated with a discrepancy between oxygen delivery (DO_2), oxygen consumption (VO_2), and a deficit in oxygen extraction (ExO_2) at the cellular level. The basic concept of organ-protective therapies is therefore to increase oxygen uptake and transport, providing an adequate supply to meet subcellular oxygen demand (1, 2). Still, the currently-used respiratory- and circulatory-supportive modalities cannot always improve sepsis-induced alterations at the later stages, and it has been suggested that the interconnected processes lead to a combined microcirculatory and mitochondrial distress syndrome, which is believed to mediate end-organ damage (3). In addition, the failing microcirculation cannot provide sufficient DO_2, and the insufficiency of the mitochondrial electron transport system (ETS) cannot sustain the adequate aerobic metabolism of the organs (3). In recent years, the bi-directional interaction between the microcirculation and mitochondria has become a focus of investigations, and it has grown increasingly apparent to date that the mechanisms involved in microcirculatory and mitochondrial dysfunction are different from those implicated in the development of macrohemodynamic changes (3, 4).

With this background, the major goal of our study was to design an adjunctive approach by which to influence the microcirculation-linked oxygen debt and energy deficit of the tissues during the late septic response. Specifically, we tested the hypothesis that the manipulation of potentially vasodilating local forces may play a role in the resuscitation of the microcirculation and the mitochondrial respiration as well. We have taken into account previous findings that elevated endothelin-1 (ET-1) levels correlate with the severity and mortality of sepsis both in animals and humans (5, 6). The members of the endothelial ET family are key peptide regulators of circulation, ET-1 being the major isoform among them

(7, 8). ET-1 effects are mediated by at least two types of G-protein-coupled receptors: the ET_A receptor (ET_A-R) mediates vasoconstriction, while the ET_B receptor (ET_B-R) mediates vasoconstriction (ET_{B2}-R subtype) and vasodilation (ET_{B1}-R subtype) (9). The ETs and ET receptors are involved in inflammatory events as well (10), and, more importantly, ET_A-R antagonist treatments have potential therapeutic benefits in experimental sepsis (11) and ischemia-reperfusion (IR)-induced microcirculatory insufficiency (12). The functional role of ET_{B1}-R is less clear. However, the stimulation of the ET_{B1}-R also provides tissue protection in pro-inflammatory and IR conditions in the peripheral and central nervous system (CNS) (13), and this activity may also have relevant peripheral microcirculatory effects through an influence on the reuptake of ET-1 (8).

Based on these findings, we hypothesized that a joint modulation of ET_A-R- and ET_{B1}-R transmitted effects may have an influence on microcirculatory recruitment and mitochondrial respiration as well. These reactions have not yet been studied in the setting of sepsis. We therefore examined the individual and combined effects of ET_A-R antagonism and selective ET_{B1}-R activation on oxygen dynamics, macro- and microcirculation, and mitochondrial ETS function in a clinically-relevant rodent model of sepsis (14).

MATERIALS AND METHODS

Animals

Male Sprague Dawley rats (350 ± 30 g) were used. The animals were housed in plastic cages (21–23°C) with a 12/12h dark-light cycle and access to standard rodent food and water *ad libitum*. The experiments were performed in accordance with National Institutes of Health guidelines on the handling and care of experimental animals and EU Directive 2010/63 for the protection of animals used for scientific purposes (approval number V/175/2018).

Preparation of polymicrobial inoculum

Polymicrobial sepsis was induced with an intraperitoneally (ip)-administered fecal inoculum. Briefly, 4 g of fresh rat feces was collected from different animals and suspended in 5 mL saline. The suspension was divided into 1 mL units, completed with sterile saline to 4 mL and incubated in water bath for 6 h at 37°C. Three mL incubated suspension (37°C) was filtered and mixed in 1 mL of agarose (2%). The concentration of the microorganisms in the suspension was determined (CFU mL^{-1}) and 1.3 mL (~0.6 mg kg^{-1}) of the mixture was injected ip for sepsis induction. There was no 48h mortality with these ip doses in pilot tests.

Experimental protocol

The animals were randomly assigned into sham-operated (Group 1, n=10) and septic (Groups 2–5) experimental groups. Fecal peritonitis was induced in the septic groups, while the sham-operated animals received an equal amount of sterile saline ip. All the animals received 1.5 mL kg^{-1} crystalloid solution 6 h later subcutaneously to maintain fluid balance (Ringerfundin®, B. Braun, Melsungen, Germany) and an analgesic agent (Buprenorphine, 15 µg kg^{-1}, Richter Pharma, Hungary). A standardized scoring system was used 6 and 22 h after sepsis induction to assess the health status of the animals and to characterize the progression of sepsis (Supplementary Digital Content - Figure 1, http://links.lww.com/SHK/A918) (15, 16). Twenty-two hours after induction, the animals were anesthetized with an ip mixture of ketamine (45.7 mg kg^{-1}) and xylazine (9.12 mg kg^{-1}) to start the invasive hemodynamic monitoring. After a 30-min recovery period and baseline measurements, the septic animals were randomly allocated into one or another of the following groups. Group 2 served as a vehicle-treated septic control and received 1 mL of saline (n=13). The next groups of septic animals received the ET_A-R antagonist ETR-p1/fl peptide (100 nmol kg h^{-1}; Kurabo Ltd., Osaka, Japan; Group 3; n=11) (17) or the highly selective ET_{B1}-R agonist [N-Succinyl-[Glu9,Ala11,15]endothelin1] (IRL-1620; 0.55 nmol kg^{-1} h^{-1}; Sigma-Aldrich, St. Louis, MO,

USA; Group 4; n=11) (9). Group 5 received a combination of the ET_A-R antagonist and ET_{B1}-R agonist compounds in the same doses (n=10). The selection of doses was based on previously reported literature data (10, 11). All treatments were administered in a continuous 60-min iv infusion in 1 mL volume, and this period was followed by an additional 30-min observation (Figure 1). Four animals were lost during surgical instrumentation due to respiratory/circulatory failure (n=1 in Sepsis + ETR-p1/fl peptide group, n=1 in Sepsis + IRL 1620 group, and n=2 in Sepsis + ETR-p1/fl peptide+ IRL 1620 group).

Surgical preparation and hemodynamic measurements

The anesthetized rats were placed in a supine position on a heating pad (37°C). A tracheostomy was performed to provide spontaneous breathing, and the right jugular vein was cannulated for continuous anesthesia (ketamine 12 mg kg^{-1} h^{-1}, xylazine 2.4 mg kg^{-1} h^{-1}, and diazepam 0.576 mg kg^{-1} h^{-1}), drug treatments, and infusion (Ringerfundin B. Braun; 10 mL kg h^{-1}). The left carotid artery was cannulated to record the mean arterial pressure (MAP) and heart rate (HR). A thermistor-tip catheter was positioned into the contralateral carotid artery to measure core temperature and cardiac output (CO) using a thermodilution technique (SPEL Advanced Cardiosys 1.4, Experimetria Ltd., Budapest, Hungary). CO was indexed for bodyweight, while total peripheral resistance (TPR) and stroke volume index (SVI) were calculated according to standard formulas (TPR=MAP CO^{-1}; SVI=CO HR^{-1}). At the end of hemodynamic monitoring, arterial and venous blood samples were taken for blood gas analysis (Cobas b121, Roche Ltd., Basel, Switzerland). The DO_2 (=CO x [(1.38 x Hb x SaO_2) + (0.003 x PaO_2)]); VO_2 (= CO x [(1.38 x Hb x (SaO_2- SvO_2)) + (0.003 x PaO_2)]); and ExO_2 (=DO_2 VO_2^{-1}) values were calculated from these parameters. The degree of lung injury was determined by using the PaO_2/FiO_2 ratio.

After the 90-min hemodynamic monitoring period, a midline abdominal incision was performed to observe the intestinal microcirculation (see later). Thereafter, a liver tissue

biopsy was taken to evaluate mitochondrial respiratory functions, followed by blood sampling for blood gases and biochemical measurements. Finally, the animals were sacrificed under deep anesthesia.

Intravital videomicroscopy

An intravital orthogonal polarization spectral imaging technique (Cytoscan A/R, Cytometrics, Philadelphia, PA) was used to visualize the serosal microcirculation of the ileum. An empty ileum segment was placed on a specially designed stage, and microcirculatory images of the serosal surface were recorded with an S-VHS video recorder 1 (Panasonic AG-TL 700, Matsushita Electric Ind. Co. Ltd., Osaka, Japan). A quantitative assessment of the microcirculatory parameters was performed offline by frame-to-frame blinded analysis of the videotaped images. Changes in red blood cell velocity (RBCV) and capillary perfusion rate (CPR; perfused/non-perfused area) in the serosal capillaries were determined in 3 separate fields by means of a computer-assisted image analysis system (IVM Pictron, Budapest, Hungary). All the microcirculatory evaluations were performed by the same investigator (R.F).

Assessment of mitochondrial respiratory function in liver homogenates

Liver samples obtained from the left lateral lobe were washed in phosphate-buffered saline and then homogenized in a medium containing 250 mM sucrose, 0.5 mM Na_2EDTA, 10 mM Tris, and 1 g L^{-1} bovine serum albumin. After homogenization, mitochondrial respiratory oxygen flux ($J_{V,O2}$; pmol $sec^{-1}mL^{-1}$) normalized to 8 mg wet weight was assessed using high-resolution respirometry (O2k, Oroboros Instruments, Innsbruck, Austria). All the measurements were performed in an MiR05 respiration medium (pH 7.1) under continuous stirring at 37°C (18). After a stable basal respiration (without exogenous substrates and ADP), NADH- and succinate-supported LEAK respiration and complex I (CI)- and complex II (CII)-linked capacities of oxidative phosphorylation (OXPHOS I and OXPHOS II) were

determined in the presence of substrates (complex I-linked: 10 mM glutamate, 2 mM malate; and complex II: 10 mM succinate) and saturating concentration of ADP (2.5 mM). Rotenone (0.5 μM), an inhibitor of CI, was administered prior to the addition of succinate to block mitochondrial ROS production via reverse electron transport. Following stimulation of OXPHOS, the integrity of the outer mitochondrial membrane was evaluated with exogenous cytochrome c (Cytc; 10 μM). ATP synthase was blocked by oligomycin (2.5 μM) to assess LEAK respiration in a non-phoshorylating state ($LEAK_{Omy}$). Respiratory control ratio (RCR), an index of coupling between respiration and phosphorylation, was expressed as a ratio of OXPHOS to $LEAK_{Omy}$ state. The ETS-independent respiration (or residual oxygen consumption; ROX) was determined following complex III inhibition with antimycin A (2.5 μM). DatLab 5.1 software (Oroboros Instruments, Innsbruck, Austria) was used for online display, respirometry data acquisition, and analysis.

Detection of inflammatory markers, metabolic and organ function injury

After the liver biopsy sampling, blood samples were taken from the inferior caval vein into precooled, EDTA-containing tubes (1 mg mL^{-1}), centrifuged (1200 g at 4°C for 10 min) and stored at -70°C until assay. Plasma levels of interleukin-6 (IL-6) and ET-1 were determined from these samples using commercial ELISA kits (Cusabio Biotechnology Ltd., Wuhan, China and Biomedica Ltd., Vienna, Austria, respectively) according to manufacturer instructions. The lactate level as an indicator of metabolic imbalance was measured from venous blood samples (Accutrend Plus Kit, Roche Diagnostics Ltd., Rotkreuz, Switzerland). Liver dysfunction was assessed by measuring plasma alanine aminotransferase (ALAT) and aspartate aminotransferase (ASAT) levels, whereas the extent of kidney injury was estimated my measuring plasma urea level using a Roche/Hitachi 917 analyzer (F. Hoffmann-La Roche AG, Switzerland). All analyses were performed on coded samples in a blinded fashion.

Statistical analysis

The sample size estimation was based on a power analysis using the PS Power and Sample Size Calculation software (version 3.1.2). Data analysis was performed with a statistical software package (SigmaStat for Windows, Jandel Scientific, Erkrath, Germany). Normality of data distribution was analyzed with the Shapiro–Wilk test. The Friedman analysis of variance on ranks was applied within groups. Time-dependent differences from the baseline for each group were assessed with Dunn's method. Differences between groups were analyzed with the Kruskal–Wallis one-way analysis of variance on ranks, followed by Dunn's method. Median values and 75^{th} and 25^{th} percentiles are provided in the figures; *P* values <0.05 were considered significant.

RESULTS

Hemodynamic changes

In the sham-operated group, there were no significant hemodynamic changes during the observation period. Sepsis, however, was accompanied by a significant hypotension (as evidenced by a temporary, approx. < 10% reduction in MAP at t=60 min, an approx. 10% increase in CO at the 60^{th} and 90^{th} min of the observation period ($P < 0.05$), and a >20% ($P < 0.05$) decrease in TPR at t=60 min (Figure 2ACD). As compared to the vehicle-treated septic group, ETR-p1/fl treatment caused a non-significant elevation in the SVI (a heart rate-independent increase in blood flow), while IRL-1620 significantly increased the MAP (by >30% at t=60 min vs t=0 min, $P < 0.05$) and TPR (by >50% at t=60 min vs t=0 min, $P < 0.05$) and decreased CO (by approx. 10% at t=60 min vs sepsis at t=60 min, $P < 0.05$) during the 90-min observation period. The combined ET_A-R antagonism and ET_{B1}-R agonism caused significant increases in MAP and TPR values as compared to the baseline and to the respective values of the vehicle-treated sepsis group (Figure 2).

Changes in oxygen dynamics

The 24-h septic period caused significant changes in oxygen dynamics, including an approx. 30% increase in DO_2 ($P < 0.05$; Figure 3A), deterioration in VO_2 (by >25%, $P < 0.05$), and a >30% reduction in ExO_2 values ($P < 0.05$) (Figure 3B-C) as compared to the sham-operated group. VO_2 and ExO_2 were significantly higher (by >35% and by nearly 50%, respectively, $P < 0.05$) after ETR-p1/fl treatment as compared to the non-treated sepsis group. A significant increase in ExO_2 was also observed in response to IRL-1620 treatment (by nearly 50%) in comparison with that of the vehicle-treated sepsis group. When these treatments were combined, the oxygen dynamics parameters were not significantly different from those of the sham-operated group, and there was a statistically non-significant trend of improvement as compared to the non-treated sepsis group (Figure 3).

Metabolic changes and organ dysfunctions

Plasma ALAT activity and urea levels were significantly higher in the non-treated septic group as compared to the sham-operated animals (by nearly 70% and >30%, respectively, $P < 0.05$) (Figure 4A-B). Lung injury, characterized by the PaO_2/FiO_2 ratio, was significantly lower (by approx. 25%, $P < 0.05$) in the septic animals (Figure 4C). The ETR-p1/fl treatment or IRL-1620 treatment did not influence the sepsis-induced changes in plasma ALAT or urea levels and the PaO_2/FiO_2 ratio (Figure 4A–C). However, when the ET_A-R antagonists and ET_{B1}-R agonists were combined, the plasma ALAT level was significantly lower than in the vehicle-treated septic group (Figure 4A). Similar changes were observed in ASAT levels (data not shown).

Likewise, polymicrobial sepsis was associated with significantly increased lactate levels (by >185%, $P < 0.05$) in the saline-treated sepsis group. In response to the ETR-p1/fl and the combined treatments, the lactate values were not different from those of the sham-operated group (Figure 4D).

Microcirculatory changes

The 24-h septic insult caused significant microcirculatory deterioration in the intestinal serosa. The CPR reached 55%, while RBCV was approx. 60% lower than those in the sham-operated animals (Figure 5A–B). When compared to the vehicle-treated sepsis group, ETR-p1/fl therapy caused a significant improvement in CPR (the values were close to those of the sham-operated group), but not in RBCV. Agonism of the ET_{B1}-R with IRL-1620 caused a slight, non-significant perfusion recovery without affecting changes in RBCV. A combination of the ETR-p1/fl and IRL-1620 treatments, however, was effective in restoring both parameters of the intestinal microcirculation (Figure 5A–B).

Changes in inflammatory markers

In the case of sepsis, plasma IL-6 and ET-1 levels reached higher values in comparison with those of the sham-operated group (by >340% and >135%, respectively, $P < 0.05$) (Figure 5C–D). IRL-1620 did not influence the sepsis-induced elevations in IL-6 and ET-1, but ETR-p1/fl treatment caused a significant reduction in plasma ET-1 level (by nearly 35%, $P < 0.05$). The combined therapy significantly reduced the sepsis-induced elevation in plasma ET-1 and reduced IL-6 values as well (P=0.051).

Changes in mitochondrial function

Intra-abdominal sepsis significantly decreased substrate oxidation as compared to the sham operation. In comparison with the vehicle-treated sepsis group, the ET_A-R antagonist and ET_B-R agonist therapies resulted in an increasing tendency in $J_{V,O2}$, and this change was statistically significant after the combination of therapies (data not shown). As a result of septic insult, both Complex-I and Complex-II-linked OXPHOS capacity and RCR values were significantly lower (by approx. 40% and 70%, respectively, $P < 0.05$) than those in the sham-operated animals (Figure 6). In comparison with the non-treated sepsis group, ETR-p1/fl treatment completely restored both CII-linked RCR and OXPHOS values (Figure 6B-D)

whereas IRL-1620 had no considerable effect on these parameters. In response to the combined treatment, however, all of the examined parameters were restored to the values of the sham-operated group (Figure 6). Sepsis resulted in significant disintegration of the outer membrane based on the effect of exogenous Cytc, but preserved membrane integrity was observed in the animals subjected to the combined treatment (Supplementary Digital Content Figure 2, http://links.lww.com/SHK/A919).

DISCUSSION

This is the first study to investigate the microcirculatory and mitochondrial consequences of a combined ET_A-R antagonist–ET_{B1}-R agonist treatment regimen in experimental sepsis. The protocol was designed in adherence with the recommendations of the Minimum Quality Threshold in Pre-clinical Sepsis Studies (MQTiPSS) guidelines with respects to proper analgesia, fluid resuscitation, temperature control, and humane endpoints (16). Systemic inflammatory activation, hemodynamic- and microcirculatory derangements, an imbalance between DO_2 and VO_2 and a reduced ExO_2, organ dysfunctions and hepatic mitochondrial dysfunction was evident 24 h after sepsis induction. In this condition, the ET_A-R antagonist treatment exerted no major influence on systemic hemodynamics, but effectively improved oxygen dynamics, ameliorated splanchnic microcirculatory dysfunction and restored the sepsis-induced CII-linked mitochondrial respiration. Supporting other findings, some of these effects can be linked to reduced inflammation (10, 19) and vasodilator effect of the ET_A-R antagonism (20).

When the modulation of the sepsis-activated ET system was tested with the ET_B-R agonist IRL-1620, the reduction in MAP and TPR was effectively counteracted and furthermore, the treatment improved oxygen dynamics and the intestinal capillary perfusion as well. These findings may be explained by the tissue-dependent vasodilator- or vasoconstrictor property of this compound, which can be linked to the subtypes of ET_B-Rs. Although it is known that

ET_{B2}-Rs have a long-lasting vasopressor effect possibly due to dominant ET_A-R activity (13, 21–23), IRL-1620 shows higher affinity to the ET_{B1}-Rs, which are expressed by the vascular endothelium and mediate nitric oxide-dependent vasodilatation (9). The beneficial effects of ET_B-R agonism have already been demonstrated in acute and chronic CNS disorders (13, 21) and in the peripheral circulation as well, possibly linking these reactions to vasodilator effects (22, 24).

In the next step in the research procedure, we examined the combined ET_A-R antagonist and ET_{B1}-R agonist therapy on the macro- and microhemodynamics and the main components of the cellular energy-providing mechanism. Combining the treatments resulted in an additive effect along the global oxygen supply–demand imbalance, and the microcirculatory parameters improved further. As a final result, organ dysfunction was significantly attenuated. We assume that reduced ET-1 levels caused by the combined treatment may play a significant role in these processes by two potential mechanisms: first, ETR-P1/fl is an intramolecular complementary peptide of the ET_A-R and can specifically bind and block ET-1 in the circulation (25). Second, activation of the ET_{B1}-R stimulates the reuptake of circulating ET-1 (8, 23).

Restoration of tissue perfusion and subcellular oxygen utilization are fundamental goals in sepsis therapy (3, 26). Vasodilator manipulation of the microcirculation can open the shunted or closed microcirculatory units and improve the imbalance between tissue oxygen supply and utilization (26). Indeed, there have been several trials of vasodilator therapies with contradictory results (27, 28). It has been suggested that these fiascos may stem from an indiscriminate application of vasoactive compounds without consideration for the phase of sepsis and the degree of microcirculatory dysfunction (29). The constantly recurring concern is timing and site specificity; the ideal sepsis therapy could increase the systemic driving pressure parallel to the opening of insufficient microcirculation through vasodilation (3, 29).

Our combined ET_A-R antagonist and ET_{B1}-R agonist treatment design has targeted this goal. The ET_B-Rs are heterogeneously distributed in the lungs, brain, and kidneys, with specific dual vasoactive effects, which can contribute to the fine tuning of tissue perfusion through either local endothelial vasodilation or vasoconstriction (8, 13, 30). Our results suggest that if microcirculatory failure occurs, the specific inactivation of vasoconstrictor ET_A-Rs can amplify the vasomodulator effects of circulating ET-1 through the ET_B-Rs, leading to a potentially beneficial outcome at the subcellular level. On the other hand, direct activation of ET_B-Rs can improve the capillary perfusion rate due to its local vasodilator effect or possibly through the increased microcirculatory driving pressure gradient as well.

The decisive role of mitochondrial dysfunction leading to oxygen utilization disorders has been demonstrated in various models of endotoxemia (31) and sepsis (32, 33). A progressive decline in OXPHOS and ATP depletion is usually present (32, 33), and we have also detected a decrease in ADP-stimulated respiration 24h after sepsis induction. The over 10% increase in oxygen flux after exogenous Cytc administration demonstrated that the outer mitochondrial membrane was injured in the septic animals (34). This change in membrane integrity may contribute to reduced ADP-ATP conversion coupled to the ETS resulting decreased RCR values. Due to the fact that a marked elevation in lactate was present, it may well be that a metabolic switch from oxidative phosphorylation to glycolysis (the Warburg effect) was present (35). In this scenario, the sepsis-associated decrease in substrate oxidation and OXPHOS was ameliorated by ET_A-R antagonist treatment. Moreover, the coupling between respiration and phosphorylation was improved, and the functional damage to the outer membrane was also mitigated.

The precise molecular mechanism by which ETR-P1/fl exerted its mitochondrial effects is not known, but the regulation of Ca^{2+} homeostasis is a plausible mechanism. The ET receptors were thought to be typical G-protein-coupled plasma membrane receptors with an

intracellular signaling cascade, but Bkaily et al. recently demonstrated ET_B-Rs in the nuclear membrane, suggesting more complicated intracellular mechanisms than was presumed previously (36). The activation of intracellular ET_B-Rs can lead to an opening of R-type calcium channels and Na^+/Ca^{2+} exchangers (NCX), which can separately raise the intranuclear and cytoplasmatic Ca^{2+} levels and establish a complex intracellular Ca^{2+} homeostasis. If ET-1 has such extensive intracellular effects on ion fluxes, mitochondria might be part of this mechanism. Accumulation of Ca^{2+} exceeding a critical threshold (~50 μM) may lead to OXPHOS failure, an opening of the mitochondrial permeability transition pore, and a depolarization of the inner mitochondrial membrane, which can ultimately lead to cell death (37). ET-1 was found to increase both cytosolic Ca^{2+} transient (38) and mitochondrial ROS production (39) and to enhance the consumption of ATP (40). It has been demonstrated that inhibition of ET_A-Rs markedly decreased mitochondrial Ca^{2+} deposition (41) and attenuated abnormalities in Ca^{2+} sequestration (42).

Interestingly, IRL-1620 alone did not significantly affect the key indices of mitochondrial respiratory function. The question arises whether the marked improvement in ADP-stimulated respiration after combined treatment is due to the modulation ET_A-Rs solely or both the ET_A-Rs and ET_{B1}-Rs. Despite the fact that IRL-1620 itself was not effective, an indirect action through the improvement of O_2 delivery/extraction cannot be ruled out. A more effective O_2 extraction in the tissues provides better O_2 diffusion to mitochondria, where it can be reduced by the ETS to support ATP synthesis (43). However, it remains unclear whether the recovery of mitochondrial function mediated by the modulation of ET receptors is *(1)* a consequence of an improved microcirculatory dysfunction, *(2)* a direct action on the organelle, or *(3)* a result of both mechanisms at the same time. The direct mitochondrial effect of ET-1 on elevated mitochondrial ROS production has been reported previously (39). Nevertheless, the presence of ET receptors has only been confirmed in the

nucleus to date. If the receptor were located on other organelles, e.g. the mitochondria or endoplasmic reticulum, this would influence various signaling processes, such as calcium transport, respiration, or apoptosis (44).

Despite compartmentalization, the microcirculatory and mitochondrial functions are closely linked under physiological circumstances. The common denominator of both mechanisms may be the capillary-mitochondrial oxygen gradient, which may be a decisive factor in mitochondrial function in sepsis. Therefore, ET receptors could indirectly influence mitochondrial function through the mechanism of tissue perfusion and restoration of the intracellular oxygen supply. The results collectively suggest that the specific ET receptor agonist and antagonist therapies used in our experiment, individually and in combination, improved the intestinal microcirculation by direct vasodilation and indirectly improved mitochondrial functions by restoring tissue perfusion and DO_2 to cells.

Limitation of the study

We attempted to follow all aspects of the MQTiPSS guidelines, but antimicrobial therapy, one of the standard treatment modalities in clinical practice, was omitted from the protocol due to the known influence of these compounds on mitochondrial respiration (45). Furthermore, we used male rats only; thus, gender-specific effects of the treatments cannot be ruled out, and a mixed population with female animals should also be used in future test studies. Further, the timeline of the examination window was relatively short; therefore, other important end-points, such as mortality, should also be investigated in longer follow-up studies or in sepsis models with increased severity.

CONCLUSION

The selective ET_B-R agonist countervailed the peritonitis-induced hypotension, while the ET_A-R antagonist maintained microcirculation and oxygen dynamics. A mixed ET receptor-targeted treatment regime may offer a novel possibility for a simultaneous microcirculatory

and mitochondrial resuscitation strategy by also reducing circulating ET-1 levels and ameliorating inflammatory indices of sepsis. Clearly, the direct relevance to human sepsis is uncertain, but these findings do highlight that ET_A-R– ET_{B1}-R-centered therapies may influence the peripheral microcirculation, which may subsequently reverse the mitochondrial dysfunction and perhaps the intracellular oxygen supply–demand mismatch.

AKNOWLEDGMENTS

The authors are grateful to Prof. Hidechika Okada (Nagoya City University, Nagoya, Japan) for providing the ETR-p1/fl peptide. Sources of funding: NKFIH K116689, GINOP-2.3.2-15-2016-00034, EFOP-3.6.2-16-2017-00006, and the UNKP-18-2 New National Excellence Program at the Hungarian Ministry of Human Capacities. This research was conducted with the support of the Szeged Scientists Academy under the sponsorship of the Hungarian Ministry of Human Capacities (EMMI:13725-2/2018/INTFIN).

REFERENCES

1. Singer M, Deutschman CS, Seymour CW, Shankar-Hari M, Annane D, Bauer M, Bellomo R, Bernard GR, Chiche JD, Coopersmith CM, et al.: The Third International Consensus Definitions for Sepsis and Septic Shock (Sepsis-3). *J Am Med Assoc* 315(8):801–810, 2016.
2. Armstrong BA, Betzold RD, May AK: Sepsis and septic shock strategies. *Surg Clin North Am* 97(6):1339–1379, 2017.
3. Balestra GM, Legrand M, Ince C: Microcirculation and mitochondria in sepsis: getting out of breath. *Curr Opin Anaesthesiol* 22(2):184–190, 2009.
4. De Backer D, Orbegozo Cortes D, Donadello K, Vincent J-L: Pathophysiology of microcirculatory dysfunction and the pathogenesis of septic shock. *Virulence* 5(1):73–79, 2014.
5. Pittet JF, Morel DR, Hemsen A, Gunning K, Lacroix JS, Suter PM, Lundberg JM: Elevated plasma endothelin-1 concentrations are associated with the severity of illness in patients with sepsis. *Ann Surg* 213(3):261–264, 1991.
6. Forni M, Mazzola S, Ribeiro LA, Pirrone F, Zannoni A, Bernardini C, Bacci ML, Albertini M: Expression of endothelin-1 system in a pig model of endotoxic shock. *Regul Pept* 131(1–3):89–96, 2005.
7. Yanagisawa M, Kurihara H, Kimura S, Tomobe Y, Kobayashi M, Mitsui Y, Yazaki Y, Goto K, Masaki T: A novel potent vasoconstrictor peptide produced by vascular endothelial cells. *Nature* 332(6163):411–415, 1988.
8. Davenport AP, Hyndman KA, Dhaun N, Southan C, Kohan DE, Pollock JS, Pollock DM, Webb DJ, Maguire JJ: Endothelin. *Pharmacol Rev* 68(2):357–418, 2016.
9. Brooks DP, DePalma PD, Pullen M, Gellai M, Nambi P: Identification and function of putative ET_B receptor subtypes in the dog kidney. *J Cardiovasc Pharmacol* 26(Suppl

3):S322–S525, 1995.

10. Boros M, Massberg S, Baranyi L, Okada H, Messmer K: Endothelin 1 induces leukocyte adhesion in submucosal venules of the rat small intestine. *Gastroenterology* 114(1):103–114, 1998.
11. Goto T, Hussein MH, Kato S, Daoud GA, Kato T, Kakita H, Mizuno H, Imai M, Ito T, Kato I, et al.: Endothelin receptor antagonist attenuates inflammatory response and prolongs the survival time in a neonatal sepsis model. *Intensive Care Med* 36(12):2132–2129, 2010.
12. Wolfárd A, Szalay L, Kaszaki J, Sahin-Tóth G, Vangel R, Balogh A, Boros M: Dynamic in vivo observation of villus microcirculation during small bowel autotransplantation: effects of endothelin-A receptor inhibition. *Transplantation* 73(9):1511–1513, 2002.
13. Gulati A, Hornick MG, Briyal S, Lavhale MS: A novel neuroregenerative approach using ET_B receptor agonist, IRL-1620, to treat CNS disorders. *Physiol Res* 67(Suppl 1):S95–S113, 2018.
14. Gonnert FA, Recknagel P, Seidel M, Jbeily N, Dahlke K, Bockmeyer CL, Winning J, Lösche W, Claus RA, Bauer M: Characteristics of clinical sepsis reflected in a reliable and reproducible rodent sepsis model. *J Surg Res* 170(1):e123–e134, 2011.
15. Rademann P, Weidinger A, Drechsler S, Meszaros A, Zipperle J, Jafarmadar M, Dumitrescu S, Hacobian A, Ungelenk L, Röstel F, et al.: Mitochondria-targeted antioxidants SkQ1 and MitoTEMPO failed to exert a long-term beneficial effect in murine polymicrobial sepsis. *Oxid Med Cell Longev* 2017:6412682, 2017.
16. Osuchowski MF, Ayala A, Bahrami S, Bauer M, Boros M, Cavaillon JM, Chaudry IH, Coopersmith CM, Deutschman CS, Drechsler S, et al.: Minimum Quality Threshold in Pre-Clinical Sepsis Studies (MQTiPSS): an international expert consensus initiative for improvement of animal modeling in sepsis. *Shock* 50(4):377–380, 2018.

17. Baranyi L, Campbell W, Ohshima K, Fujimoto S, Boros M, Okada H: The antisense homology box: a new motif within proteins that encodes biologically active peptides. *Nat Med* 1(9):894–901, 1995.

18. Doerrier C, Garcia-Souza LF, Krumschnabel G, Wohlfarter Y, Mészáros AT, Gnaiger E: High-resolution fluorespirometry and OXPHOS protocols for human cells, permeabilized fibers from small biopsies of muscle, and isolated mitochondria. *Methods Mol Biol* 1782:31–70, 2018.

19. Piechota-Polanczyk A, Kleniewska P, Gorąca A: The influence of ETA and ETB receptor blockers on LPS-induced oxidative stress and NF-κB signaling pathway in heart. *Gen Physiol Biophys.* 31(3):271–278, 2012.

20. Szalay L, Kaszaki J, Nagy S, Boros M: The role of endothelin-1 in circulatory changes during hypodynamic sepsis in the rat. *Shock* 10(2):123–128, 1998.

21. Gulati A: Endothelin receptors, mitochondria and neurogenesis in cerebral ischemia. *Curr Neuropharmacol* 14(6):619–626, 2016.

22. Matsuura T, Yukimura T, Kim S, Miura K, Iwao H: Selective blockade of endothelin receptor subtypes on systemic and renal vascular responses to endothelin-1 and IRL 1620, a selective endothelin ET_B-receptor agonist, in anesthetized rats. *Jpn J Pharmacol* 71(3):213–220, 1996.

23. McMurdo L, Thiemermann C, Vane JR: The endothelin ET_B receptor agonist, IRL 1620, causes vasodilation and inhibits ex vivo platelet aggregation in the anaesthetised rabbit. *Eur J Pharmacol* 259(1):51–55, 1994.

24. Honoré J-C, Fecteau M-H, Brochu I, Labonté J, Bkaily G, D'Orleans-Juste P: Concomitant antagonism of endothelial and vascular smooth muscle cell ET_B receptors for endothelin induces hypertension in the hamster. *Am J Physiol* 289(3):H1258–H1264, 2005.

25. Baranyi L, Campbell W, Ohshima K, Fujimoto S, Boros M, Kaszaki J, Okada H: Antisense homology box-derived peptides represent a new class of endothelin receptor inhibitors. *Peptides* 19(2):211–223, 1998.

26. Corrêa TD, Filho RR, Assunção MSC, Silva E, Lima A: Vasodilators in septic shock resuscitation. *Shock* 47(3):269–275, 2017.

27. Trzeciak S, Glaspey LJ, Dellinger RP, Durflinger P, Anderson K, Dezfulian C, Roberts BW, Chansky ME, Parrillo JE, Hollenberg SM: Randomized controlled trial of inhaled nitric oxide for the treatment of microcirculatory dysfunction in patients with sepsis. *Crit Care Med* 42(12):2482–2492, 2014.

28. Boerma EC, Koopmans M, Konijn A, Kaiferova K, Bakker AJ, van Roon EN, Buter H, Bruins N, Egbers PH, Gerritsen RT, et al.: Effects of nitroglycerin on sublingual microcirculatory blood flow in patients with severe sepsis/septic shock after a strict resuscitation protocol: A double-blind randomized placebo controlled trial. *Crit Care Med* 38(1):93–100, 2010.

29. Moore JPR, Dyson A, Singer M, Fraser J: Microcirculatory dysfunction and resuscitation: why, when, and how. *Br J Anaesth* 115(3):366–375, 2015.

30. Inscho EW, Imig JD, Cook AK, Pollock DM: ET_A and ET_B receptors differentially modulate afferent and efferent arteriolar responses to endothelin. *Br J Pharmacol* 146(7):1019–1026, 2005.

31. Callahan LA, Supinski GS: Sepsis induces diaphragm electron transport chain dysfunction and protein depletion. *Am J Respir Crit Care Med* 172(7):861–868, 2005.

32. Doerrier C, García JA, Volt H, Díaz-Casado ME, Lima-Cabello E, Ortiz F, Luna-Sánchez M, Escames G, López LC, Acuña-Castroviejo D: Identification of mitochondrial deficits and melatonin targets in liver of septic mice by high-resolution respirometry. *Life Sci* 121:158–165, 2015.

33. Arulkumaran N, Deutschman CS, Pinsky MR, Zuckerbraun B, Schumacker PT, Gomez H, Gomez A, Murray P, Kellum JA, ADQI XIV Workgroup: Mitochondrial function in sepsis. *Shock* 45(3):271–281, 2016.

34. Crouser ED, Julian MW, Huff JE, Joshi MS, Bauer JA, Gadd ME, Wewers MD, Pfeiffer DR: Abnormal permeability of inner and outer mitochondrial membranes contributes independently to mitochondrial dysfunction in the liver during acute endotoxemia. *Crit Care Med* 32(2):478–488, 2004.

35. Bar-Or D, Carrick M, Tanner A, Lieser MJ, Rael LT, Brody E: Overcoming the Warburg effect: Is it the key to survival in sepsis? *J Crit Care* 43:197–201, 2018.

36. Bkaily G, Choufani S, Avedanian L, Ahmarani L, Nader M, Jacques D, D'Orléans-Juste P, Al Khoury J: Nonpeptidic antagonists of ET_A and ET_B receptors reverse the ET-1-induced sustained increase of cytosolic and nuclear calcium in human aortic vascular smooth muscle cells. *Can J Physiol Pharmacol* 86(8):546–556, 2008.

37. Elustondo PA, Negoda A, Kane CL, Kane DA, Pavlov EV: Spermine selectively inhibits high-conductance, but not low-conductance calcium-induced permeability transition pore. *Biochim Biophys Acta* 1847(2):231–240, 2015.

38. Goto K, Kasuya Y, Matsuki N, Takuwa Y, Kurihara H, Ishikawa T, Kimura S, Yanagisawa M, Masaki T: Endothelin activates the dihydropyridine-sensitive, voltage-dependent Ca^{2+} channel in vascular smooth muscle. *Proc Natl Acad Sci USA* 86(10):3915–3918, 1989.

39. De Giusti VC, Correa MV, Villa-Abrille MC, Beltrano C, Yeves AM, de Cingolani GEC, Cingolani HE, Aiello EA: The positive inotropic effect of endothelin-1 is mediated by mitochondrial reactive oxygen species. *Life Sci* 83(7–8):264–271, 2008.

40. Yuki K, Suzuki T, Katoh S, Kakinuma Y, Miyauchi T, Mitsui Y: Endothelin-1 stimulates cardiomyocyte injury during mitochondrial dysfunction in culture. *Eur J Pharmacol*

431(2):163–170, 2001.

41. Mino N, Kobayashi M, Nakajima A, Amano H, Shimamoto K, Ishikawa K, Watanabe K, Nishikibe M, Yano M, Ikemoto F: Protective effect of a selective endothelin receptor antagonist, BQ-123, in ischemic acute renal failure in rats. *Eur J Pharmacol* 221(1):77–83, 1992.
42. Brunner F, Wölkart G, Haleen S: Defective intracellular calcium handling in monocrotaline-induced right ventricular hypertrophy: protective effect of long-term endothelin-A receptor blockade with 2-benzo[1,3]dioxol-5-yl-3-benzyl-4-(4-methoxy-phenyl-)- 4-oxobut-2-enoate-sodium (PD 155080). *J Pharmacol Exp Ther* 300(2):442–449, 2002.
43. Boveris DL, Boveris A: Oxygen delivery to the tissues and mitochondrial respiration. *Front Biosci* 12:1014–1023, 2007.
44. Tykocki NR, Watts SW: The interdependence of endothelin-1 and calcium: a review. *Clin Sci (Lond)* 119(9):361–372, 2010.
45. Moullan N, Mouchiroud L, Wang X, Ryu D, Williams EG, Mottis A, Jovaisaite V, Frochaux MV, Quiros PM, Deplancke B, et al.: Tetracyclines disturb mitochondrial function across eukaryotic models: a call for caution in biomedical research. *Cell Rep* 10(10):1681–1691, 2015.

FIGURE LEGENDS

Figure 1. The experimental scheme. The animals were randomly assigned into sham-operated and septic experimental groups. Twenty-two hours after sepsis induction, the animals were divided into 4 subgroups: treated with saline, the ET_A receptor antagonist ETR-p1/fl peptide (100 nmol kg^{-1} h^{-1} iv), the ET_{B1} receptor agonist IRL-1620 (0.55 nmol kg^{-1} h^{-1} iv), or the same doses as the combination therapy.

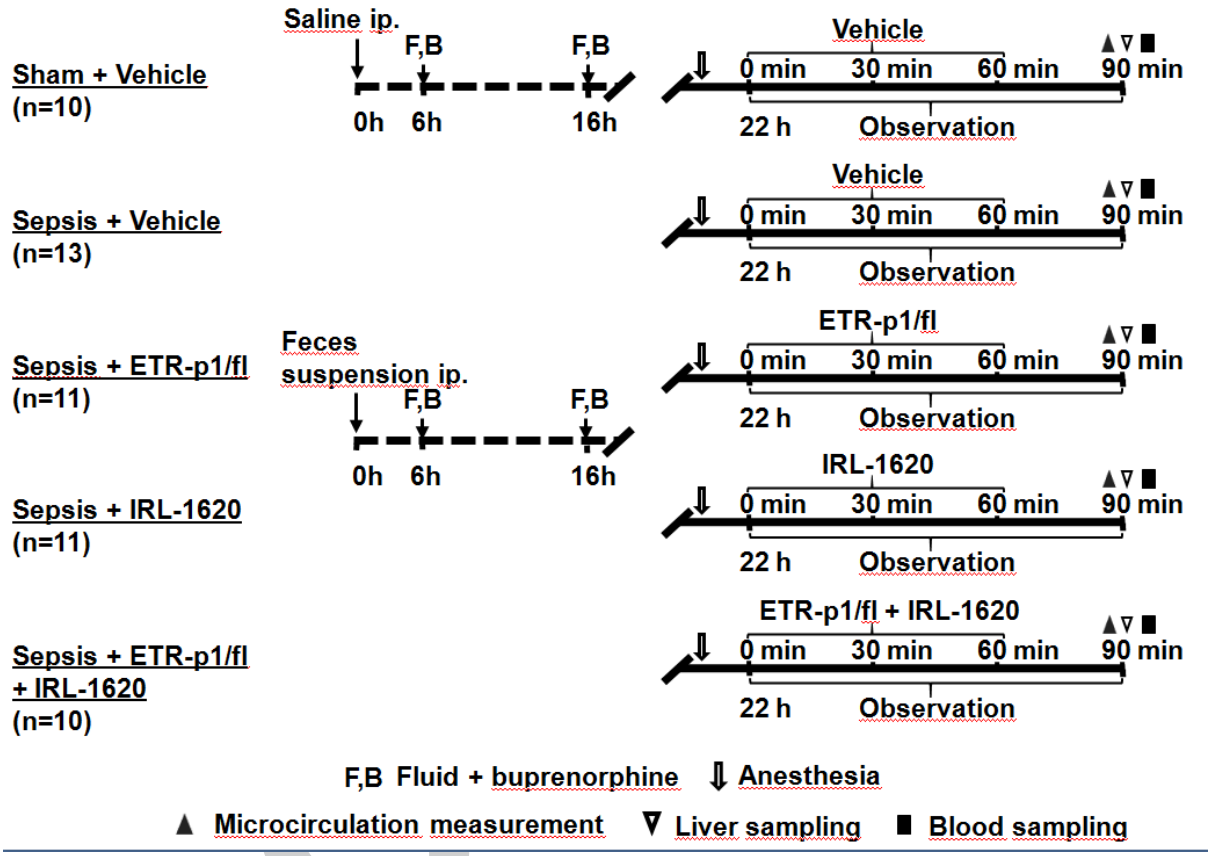

Figure 2. Changes in mean arterial pressure (A), stroke volume index (B), cardiac output (C), and total peripheral resistance response (D) in the sham-operated group (open circles) and in the different sepsis groups treated with saline vehicle (black triangle), the ET_A receptor antagonist ETR-p1/fl (grey square), the ET_{B1} receptor agonist IRL-1620 (grey diamond), and a combination of these (black hexagon with plus sign). The plots demonstrate the median values and the 25th (lower whisker) and 75th (upper whisker) percentiles. x $P < 0.05$ vs. sham-operated; # $P < 0.05$ vs. vehicle-treated sepsis; * $P < 0.05$ vs. 0 min.

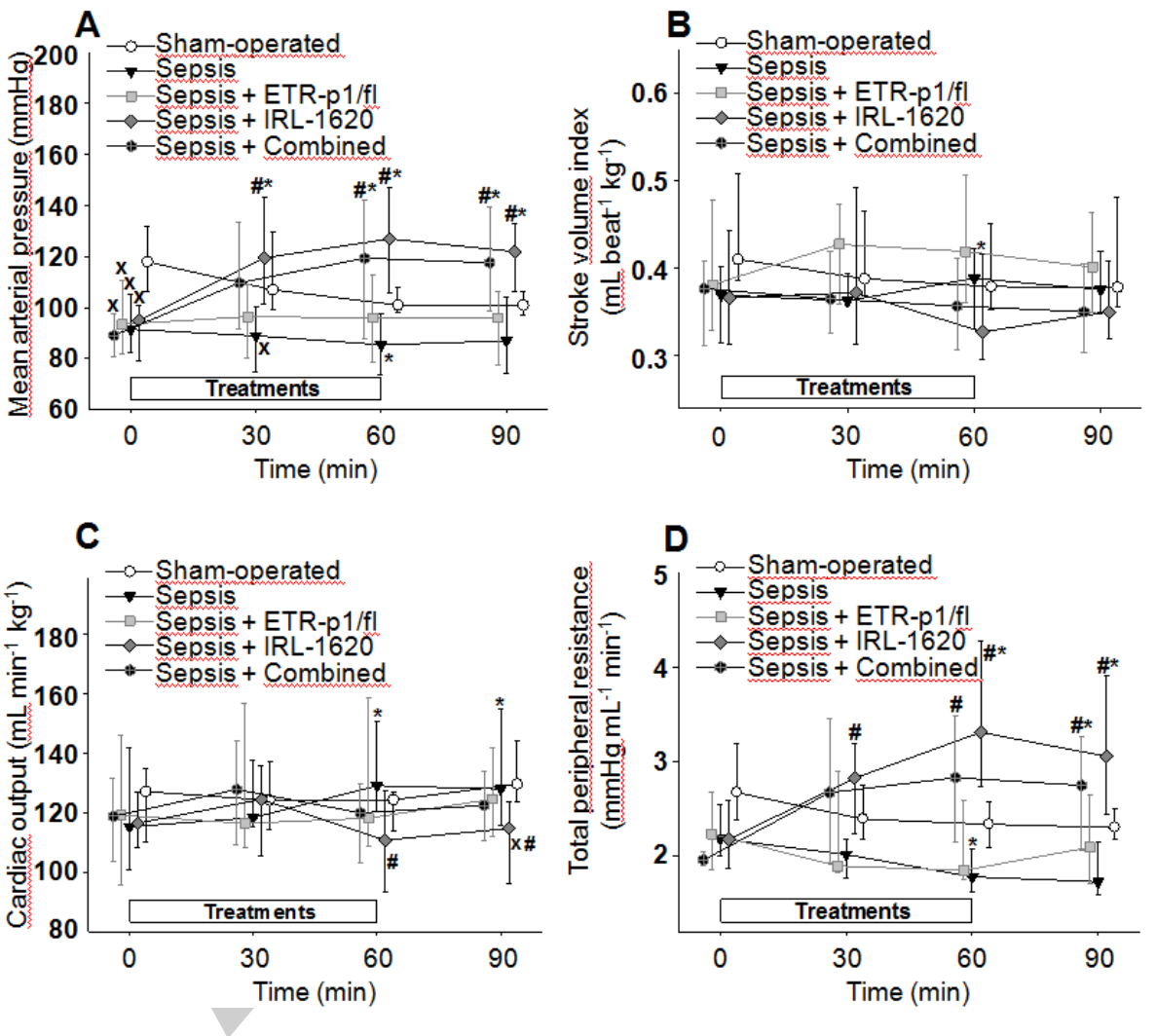

Figure 3. Oxygen delivery (DO_2) (A), oxygen consumption (VO_2) (B), and oxygen extraction (C) in the sham-operated group (empty box) and in the different septic groups treated with saline (black box), the ET_A receptor antagonist ETR-p1/fl (striped box), the ET_{B1} receptor agonist IRL-1620 (striped box), and a combination of these (checked box). The plots demonstrate the median (horizontal line in the box) and the 25th (lower whisker) and 75th (upper whisker) percentiles. Between groups: Kruskal–Wallis test and Dunn's post-hoc test. x $P < 0.05$ vs. sham-operated; # $P < 0.05$ vs. vehicle-treated sepsis.

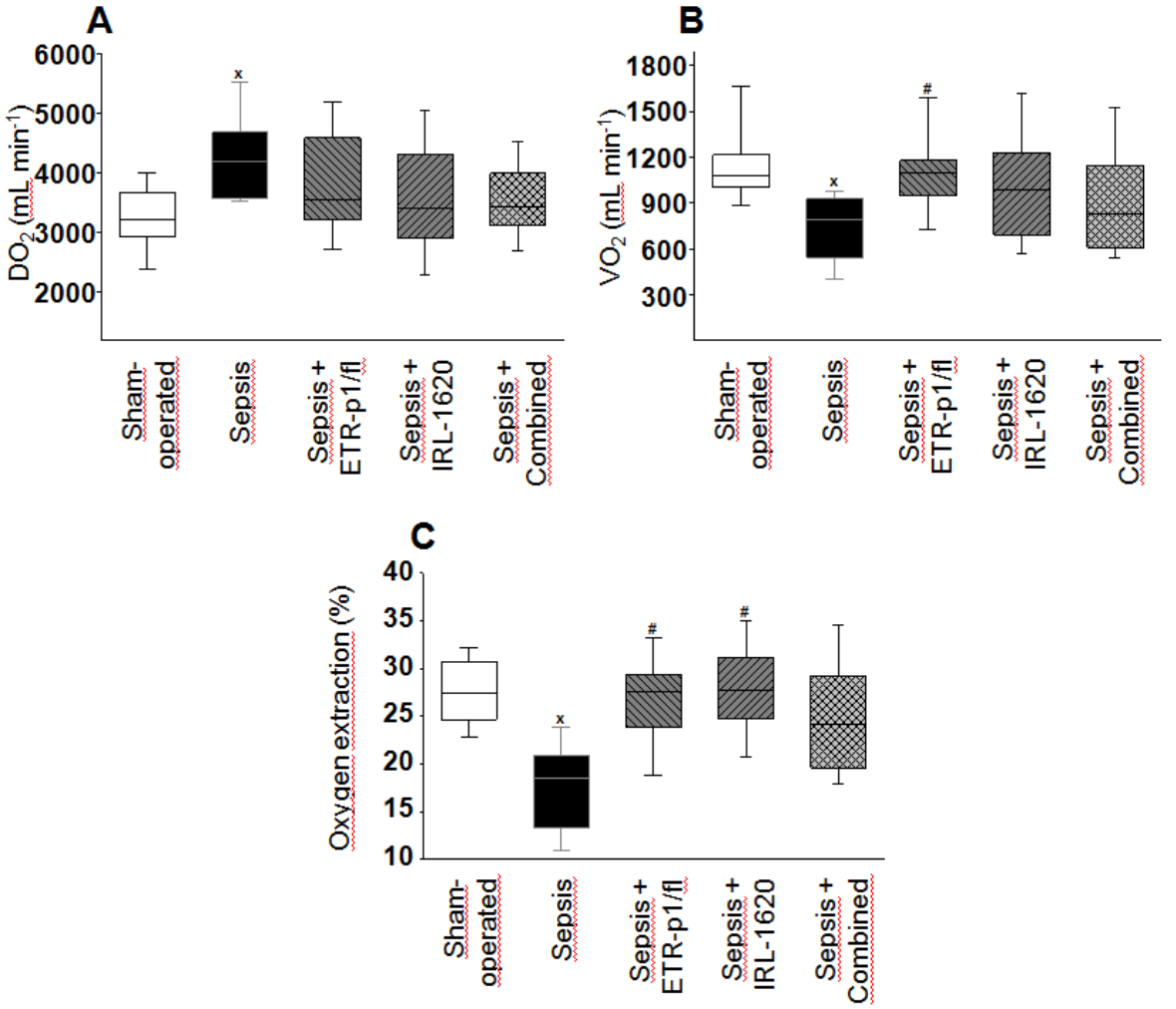

Figure 4. Plasma alanine aminotransferase (ALAT) (A), urea (B), and PaO_2/FiO_2 ratio (C) and lactate levels (D) in the sham-operated group (empty box) and in the different sepsis groups treated with saline vehicle (black box), the ET_A receptor antagonist ETR-p1/fl (striped box), the ET_{B1} receptor agonist IRL-1620 (striped box), and a combination of these (checked box). The plots demonstrate the median (horizontal line in the box) and the 25th (lower whisker) and 75th (upper whisker) percentiles. x $P < 0.05$ vs. sham-operated; # $P < 0.05$ vs. vehicle-treated sepsis.

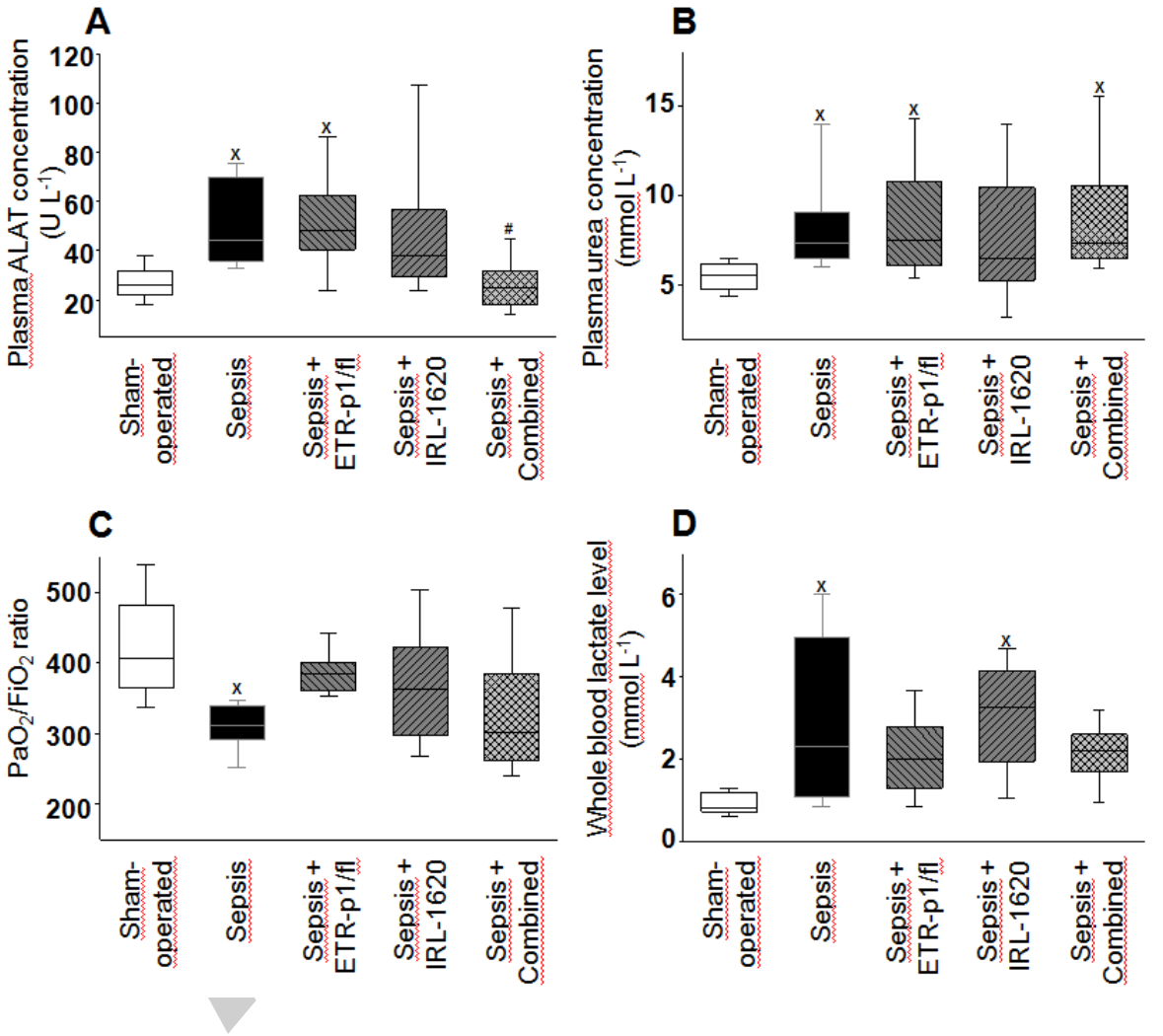

Figure 5. Capillary perfusion rate (A), red blood cell velocity (B), plasma interleukin-6 (IL-6) concentration (C), and plasma endothelin-1 (ET-1) (D) in the sham-operated group (empty box) and in the different sepsis groups treated with saline vehicle (black box), the ET_A receptor antagonist ETR-p1/fl (striped box), the ET_{B1} receptor agonist IRL-1620 (striped box), and a combination of these (checked box). The plots demonstrate the median (horizontal line in the box) and the 25th (lower whisker) and 75th (upper whisker) percentiles. Between groups: Kruskal–Wallis test and Dunn's post-hoc test. x $P < 0.05$ vs. sham-operated; # $P < 0.05$ vs. vehicle-treated sepsis.

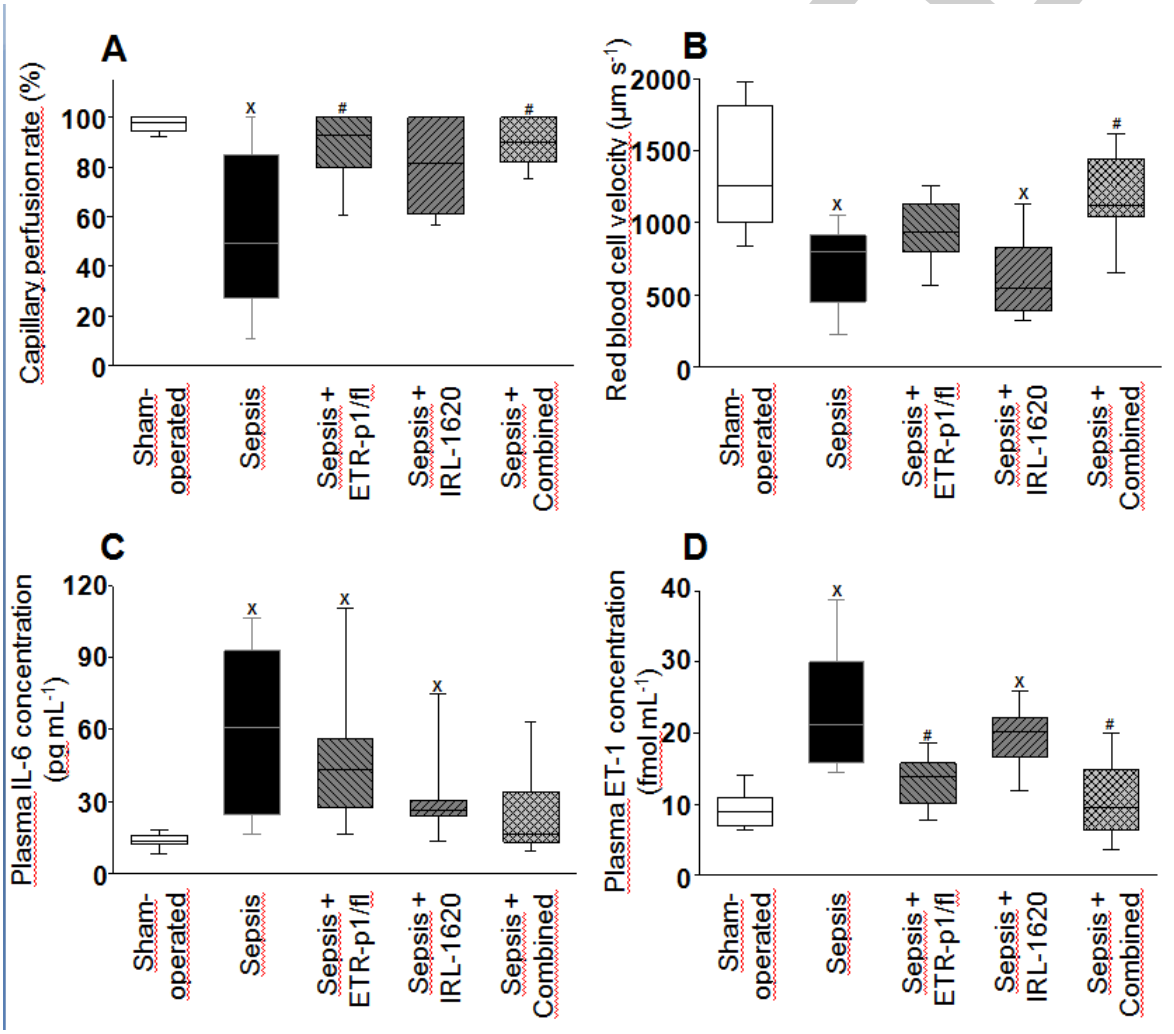

Figure 6. Complex I-linked OXPHOS capacity (C1-OXPHOS) (A), complex II-linked OXPHOS capacity (C1I-OXPHOS) (B), complex I respiration control ratio (CI-RCR) (C), and complex II respiration control ratio (CII-RCR) (D) in the sham-operated group (empty box) and in the different sepsis groups treated with saline vehicle (black box), the ET_A receptor antagonist ETR-p1/fl (striped box), the ET_{B1} receptor agonist IRL-1620 (striped box), and a combination of these (checked box). The plots demonstrate the median (horizontal line in the box) and the 25th (lower whisker) and 75th (upper whisker) percentiles. x $P < 0.05$ vs. sham-operated; # $P < 0.05$ vs. vehicle-treated sepsis.